

MECHANISM OF MICROWAVE ENERGY STORAGE IN “TRAPPED MODE” OSCILLATIONS

Zhivkov O.P., Avdieienko H. L., Krylach O. F., Stepanenko V. M.

National Technical University of Ukraine
“Igor Sikorsky Kyiv Polytechnic Institute”, Ukraine

E-mail: django2006@ukr.net

Abstract

In microwave devices performing the functions of delay lines, equalizers and information storage cells “storage” of electromagnetic oscillations energy in one or another form is realized, associated with their specific phase and time group delay characteristics. The report considers microstrip and 3-D cells of metamaterials which realizing such properties and demonstrates ways to achieve optimal parameters of these structures from the point of view of losses and “time delay”.

Introduction

Phase equalization of band-pass filters has always been an urgent task in the design of microwave devices [1-3]. In [4-6] it was demonstrated that bridge resonant structures in the form of all-pass filters are also applicable for modeling the characteristics of metamaterial cells. As described in papers [7-9] metamaterial cells are also used as storage and retrieval devices. The properties of all-pass filters based on lumped elements without taking into account losses in resonators have been well studied for a long time [10,11], but particular interest are the characteristics of this kind of lossy filters. In paper [12] it is noted that the structures with two independent channels of energy transmission belong to the so-called “non-minimal-phase” circuits, and also that this kind of circuits in the form of a bridge circuit with series and parallel oscillatory circuits in parallel and crossed arms (Fig.1(a)) are “phase-correcting units” which can provide infinite attenuation even taking into account losses in the circuits (i.e., at finite values of the Q-factor of resonance circuits). That is why this kind of bridge structures, as well as equivalent circuits shown in Fig. 1(b), can have characteristics like Fano resonance and electromagnetically induced transparency (EIT) [4-6]. It is noted there that the infinite attenuation is due to the balance of currents of different branches of the circuit in the common load. Consequently, a change in the current direction (current phase) can cause the derivative of the phase response to also change sign to the opposite and the value of the group delay time to become positive, which, as noted in [13], does not imply a violation of the principle of causality.

In modeling metamaterial cells, since the beginning of their study, ladder circuits or circuits based on coupled circuits have been traditionally used [14]. In this kind of structures, the energy from the generator to the load propagates along one channel, and the energy exchange between coupled oscillatory circuits takes place in the same “forward-backward” direction. In bridge circuits resonators can exchange energy between themselves in the “transverse” direction without affecting the oscillator and load circuits, i.e., creating the conditions of existence for the so-called “trapped” modes [6,15]. The parameters of such systems from the point of view of achievable limits of electromagnetic oscillation energy accumulation and related parameters of group delay (GD) time and insertion damping are considered below.

Theoretical Background

In [4], the S_{11} and S_{21} parameters of system with two independent resonators (oscillations) of different types, modeled by bridge equivalent circuits (Fig.1) are represented as:

$$S_{11} = K_2^*/(1 + K_2^*) - K_1^*/(1 + K_1^*), \quad (1)$$

$$S_{21} = 1 - K_1^*/(1 + K_1^*) - K_2^*/(1 + K_2^*), \quad (2)$$

where

$$K_1^* = K_1 / [(1 + j)(\xi + a)], \quad (3)$$

$$K_2^* = K_2 / [(1 + j)(\xi - a) \cdot b], \quad (4)$$

$$K_1 = Q_{01} / Q_{ext1}, \quad (5)$$

$$K_2 = Q_{02} / Q_{ext2}, \quad (6)$$

where Q_{0i} is the unloaded Q-factor of the “i” resonator, Q_{exti} is the external Q-factor of the “i” resonator ($i=1,2$); ξ is generalized frequency detuning to the central frequency of the filter f_0 , and a is generalized frequency detuning of “parallel” f_{par} and “series” f_{ser} resonators to f_0 .

$$f_0 = (f_{par} + f_{ser})/2, \quad (7)$$

$$\xi = 2(f - f_0) \cdot (Q_{01} \cdot Q_{02})^{1/2} / (f + f_0), \quad (8)$$

$$a = 2(f_{par} - f_{ser}) \cdot (Q_{01} \cdot Q_{02})^{1/2} / (f_{par} + f_{ser}), \quad (9)$$

$$b = Q_{02} / Q_{01}. \quad (10)$$

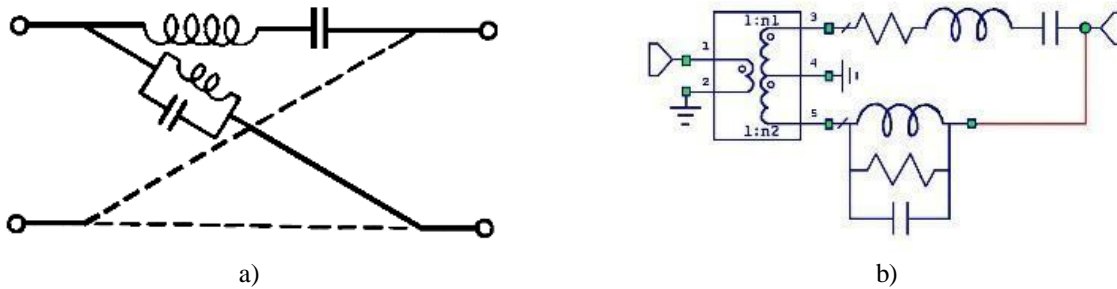


Fig. 1. The equivalent circuit of an all-pass filter a) classic structure; b) circuits with balun

Normalized total stored energy in a two-resonator system (this is sum of the energy stored by the resonant system and energy losses, including radiation losses) can be defined as:

$$E_{\Sigma} = 1 - |S_{11}|^2 - |S_{21}|^2 = 2|K_1^*|/(1+K_1^*)^2 + 2|K_2^*|/(1+K_2^*)^2 = E_1 + E_2 \quad (11)$$

and is equal, as we see, to the sum of the accumulated normalized energies E_i of individual resonators (oscillations). For an individual i -th resonator, the maximum of the accumulated energy is reached at $K_i = 1$, i.e., at the equality of its intrinsic and external Q-factor and is equal to half of the total incident energy, a quarter of the energy is reflected, and a quarter is transmitted. In a perfectly matched two-resonator system, at $K_1 = K_2 = 1$, the entire incident energy can be stored, and there will be no reflection and passage of energy (as per formulas (1), (2)).

Fig. 2 shows the transmission coefficients of individual resonators (parallel oscillating circuit - red curve, series oscillating circuit - green curve) and the transmission (S_{21}) and reflection (S_{11}) coefficients of the whole resonant system (blue curves) for resonators with the same Q-factor value. To demonstrate the almost merging green and red characteristics as well as the overall reflection curve S_{11} , the transmission coefficients for the different oscillations are slightly different ($K_1=1$; $K_2=1.1$).

A matched resonant structure of the all-pass filter type can be used as a model of the “trapped” mode of oscillations [15,16]. Trapped mode oscillations occur by energy exchange between resonant circuits in the direction which transverse to the direction of energy propagation from input to output (from generator to load). In the mode of perfect matching at $K_1 = K_2 = 1$, the characteristic of the cell transmission coefficient $S_{21} = 0$ dB at the resonant frequency and has an infinitely narrow width of the spectral line at the level of -3 dB, as well as tending to infinity value of the group delay time GD (decrement of attenuation is close to zero), so “trapped” modes are usually characterized in this case as the mode of “super-quality” oscillation.

In real microwave structures based on MSR and DR all this is realizable using at least two independent channels of energy propagation included in parallel between input and output and excited by different types of oscillations: in-phase and anti-phase, even and odd, electric and magnetic (by analogy with electric and magnetic dipoles). Such structures in the modes of Fano resonance and EIT are considered below, and their “energy” characteristics are analyzed.

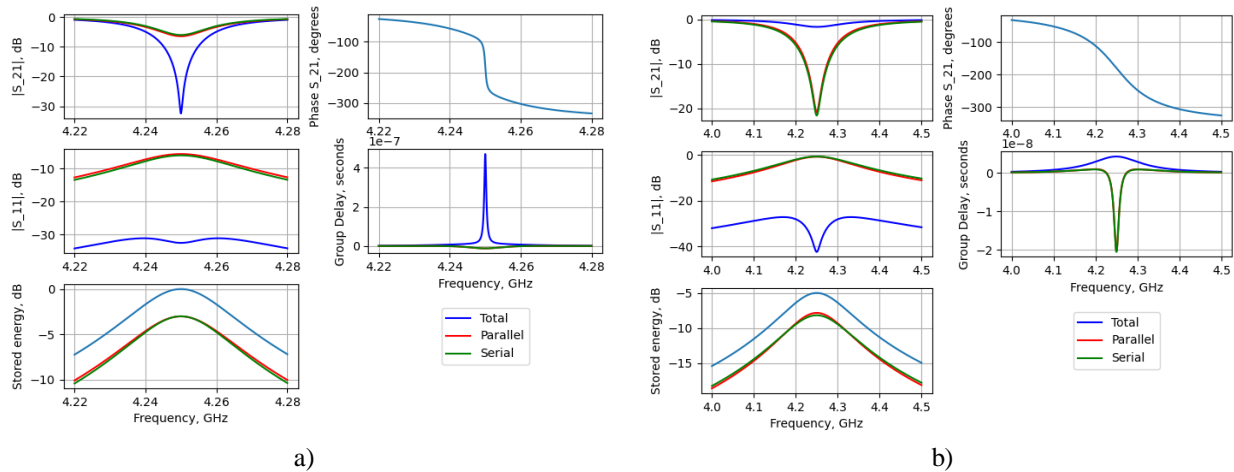


Fig. 2. Characteristics of the all-pass filter in the matching mode: a) $K_1 \approx K_2 = 1$; b) $K_1 \approx K_2 = 10$. Green curves - characteristics of the low-Q series circuit, red - characteristics of the low-Q parallel circuit, blue curves - characteristics of the whole oscillatory system

Experimental Results

Fig.3 shows the layouts of two types of metamaterial cells consisting of the combination of the microstrip (MSR) and dielectric (DR) resonators (Fig.3(a)) and combination microstrip resonators of various length (Fig.3(b)).

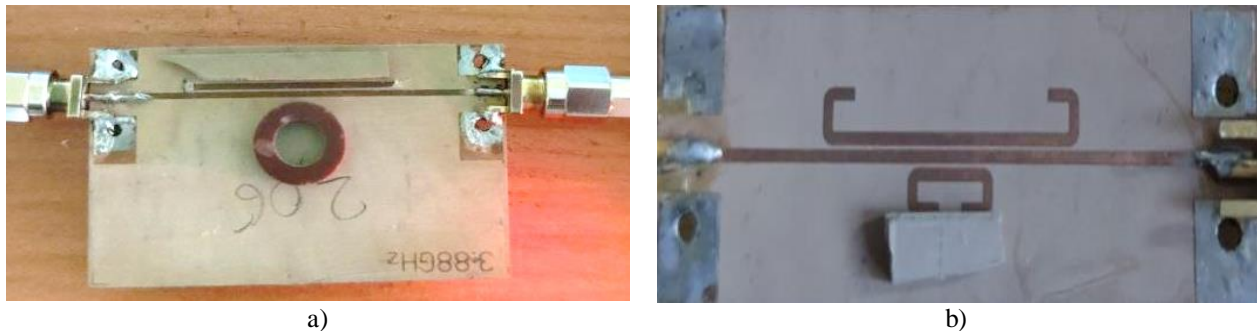
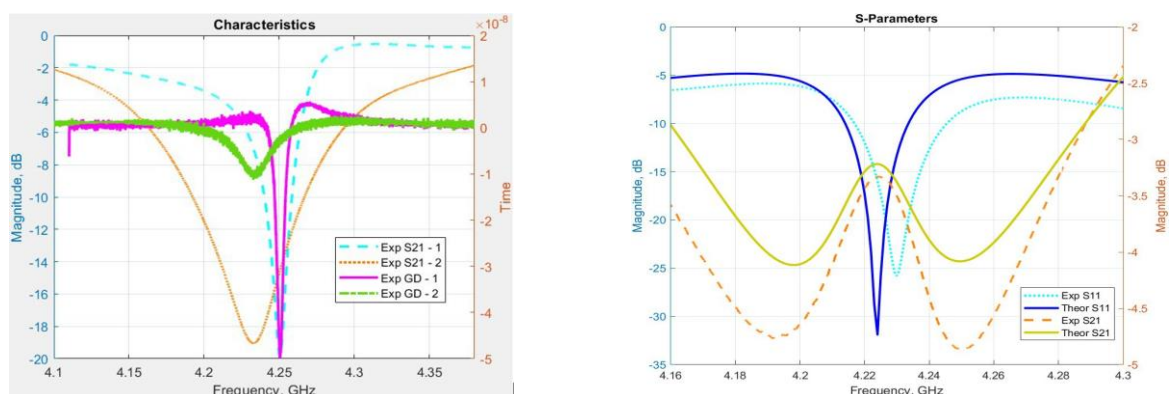


Fig.3. Photographs of layouts of the investigated filters based on metamaterial cells

Fig.4(a) shows the metamaterial cell characteristics based on the combination of the DR and MSR for the layout of Fig.3(a) measured separately for DR and MSR, such that the insertion loss levels are approximately the same (approximately -19 dB).

The higher value of Q-factor of the DR compared to the MSR is visually observed. This is also evidenced by the values of the GD parameter - of about 11 ns in the MSR and about 50 ns in the DR.



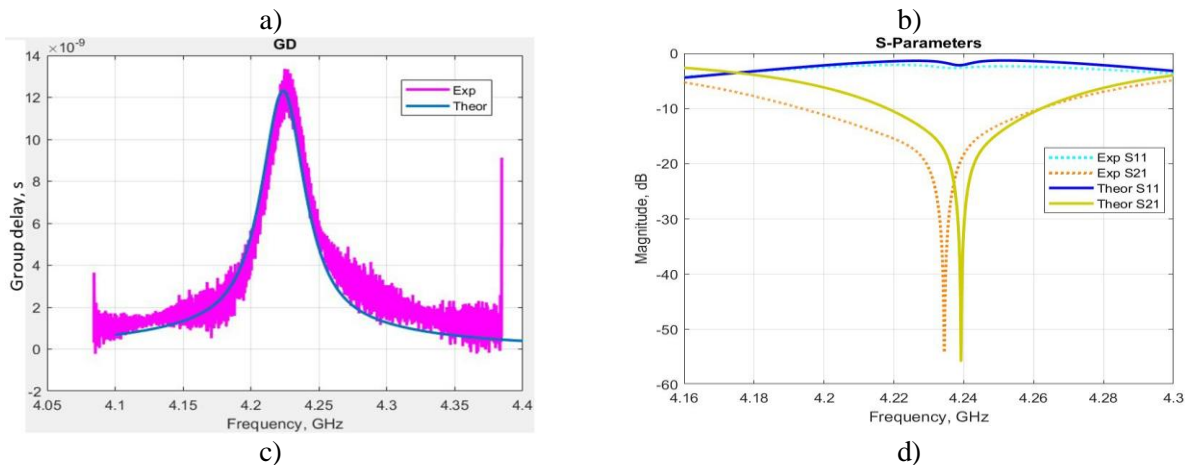


Fig.4. Frequency characteristics of metamaterial cell based on the combination of the MSR and DR for the layout of Fig.3,b: a) experimental measured S_{21} and GD (1 – DR, 2 – MSR); b) experimental and theoretic values of S_{21} parameter in the EIT mode; c) experimental and theoretic values of GD parameter in the EIT mode; d) experimental and theoretic values of S_{21} parameter in the mode of Fano resonance; e) experimental and theoretic values of GD parameter in the mode of Fano resonance

Fig.4(b)-4(c) show the characteristics of the whole metamaterial cell in the EIT (electromagnetically induced transparency) mode, and Fig.4(d)-4(e) show the “exotic” for Fano resonance variant (Fano resonance in general case has asymmetric amplitude characteristics) of coincidence of resonance frequencies of DR and MSR (resonance is achieved due to fulfillment of condition

$$K_{DR} \cdot K_{MSR} = 1 \quad (12)$$

where K_{DR} and K_{MSR} – respectively coupling coefficients of DR and MSR with the transmission line. For loss level at the resonant frequency of about -19 dB the $K_{MSR} \approx 8$ and, accordingly, removing DR from the transmission line, it was possible to ensure its weak coupling $K_{DR} \approx 0.125$ (attenuation level of about 1 dB).

The theoretical curves in Fig.4(b) – 4(e) are calculated with the following circuit parameters (Fig.1(b)) presented in Tab.1.

Table 1. Circuit Parameters

Parameters	Parallel EIT	Series EIT	Parallel Fano	Series Fano
R, Ohm	800	16.6	820	800
L, nH	0.12	717	0.1188	14320
C, pF	11.95	0.002	11.86	$9.845 \cdot 10^{-5}$

Fig.5(a) shows the frequency dependences of the stored energies calculated in accordance with (11). The red curve corresponds to the energy of the low-Q MSR, the green curve corresponds to the energy of the high-Q DR, and the blue curve characterizes the total energy of the cell (the calculation was performed for the case $K_{DR} = 6$, $K_{MSR} = 8$, which corresponds to the measured and simulated parameters S_{11} and S_{21} in the “transparency window” mode (Fig. 4(b) - 4(c)).

Fig.5(b) shows similar dependences calculated for the Fano resonance (Fig.4(e)) at the previously indicated values of $K_{MSR} = 8$ and $K_{DR} = 0.1255$. In Fig.5(a) for “Storage energy” it can be seen that in the region where the total stored energy (blue curve) exceeds by level the energy stored by individual resonators, part of it is “over-radiated” in the direction of the load (S_{21} in this region decreases, more energy is supplied to the output), and the reflection, on the contrary, decreases. Note that in the “transparency window” mode, the GD value of the cell as a whole is less than the GD of the resonators forming it, and very large GD values in the Fano resonance mode are achieved only at very high loss levels (at very weak signals). Note that the connection between steep phase characteristics of filters and large levels of attenuation has been researched for quite a long time [18].

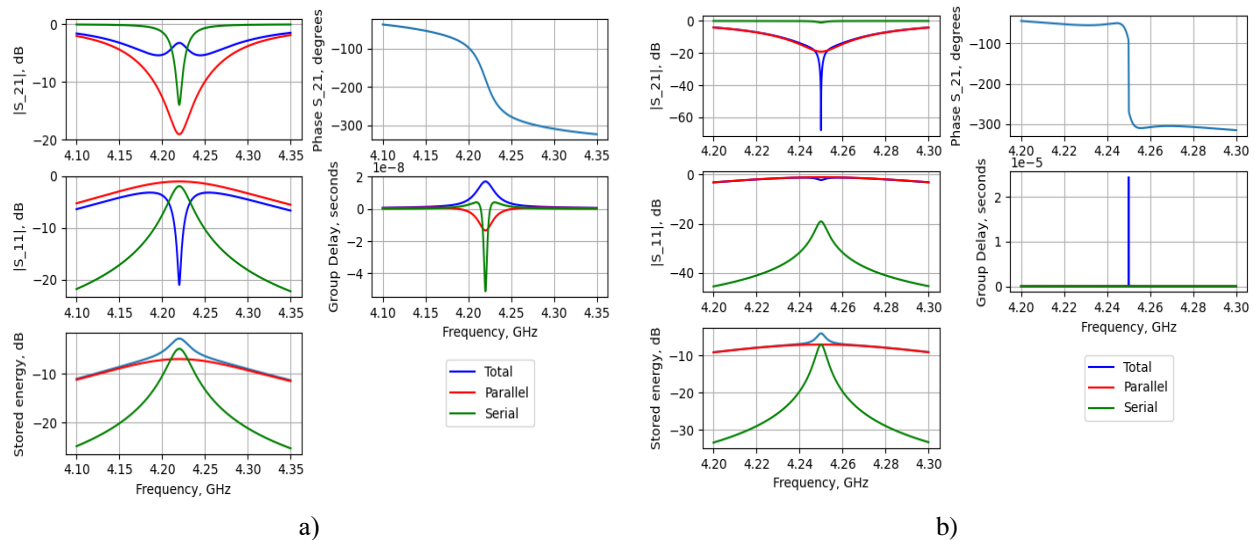


Fig. 5. Frequency characteristics (S_{21} , S_{11} , E_s , Phase, GD) of metamaterial cell: a) in the EIT mode; b) in the mode of Fano resonance

We have also studied a microstrip metamaterial cell Fig. 3(b), an analog of a standard split-ring resonator (SRR) that consists of short “inner” and long “outer” resonators. During research the resonance frequency of the smaller microstrip resonator of the metamaterial cell (Fig.3(b)) was changed using a small piece of dielectric with low dielectric permittivity by superimposing it on the resonator (the larger the size of the dielectric on the resonator, the lower its resonant frequency). The layouts of metamaterial cells are tested in the modes of minimum (transparency windows) and maximum (Fano resonance) losses. Its experimental and theoretical characteristics are presented in Fig. 6.

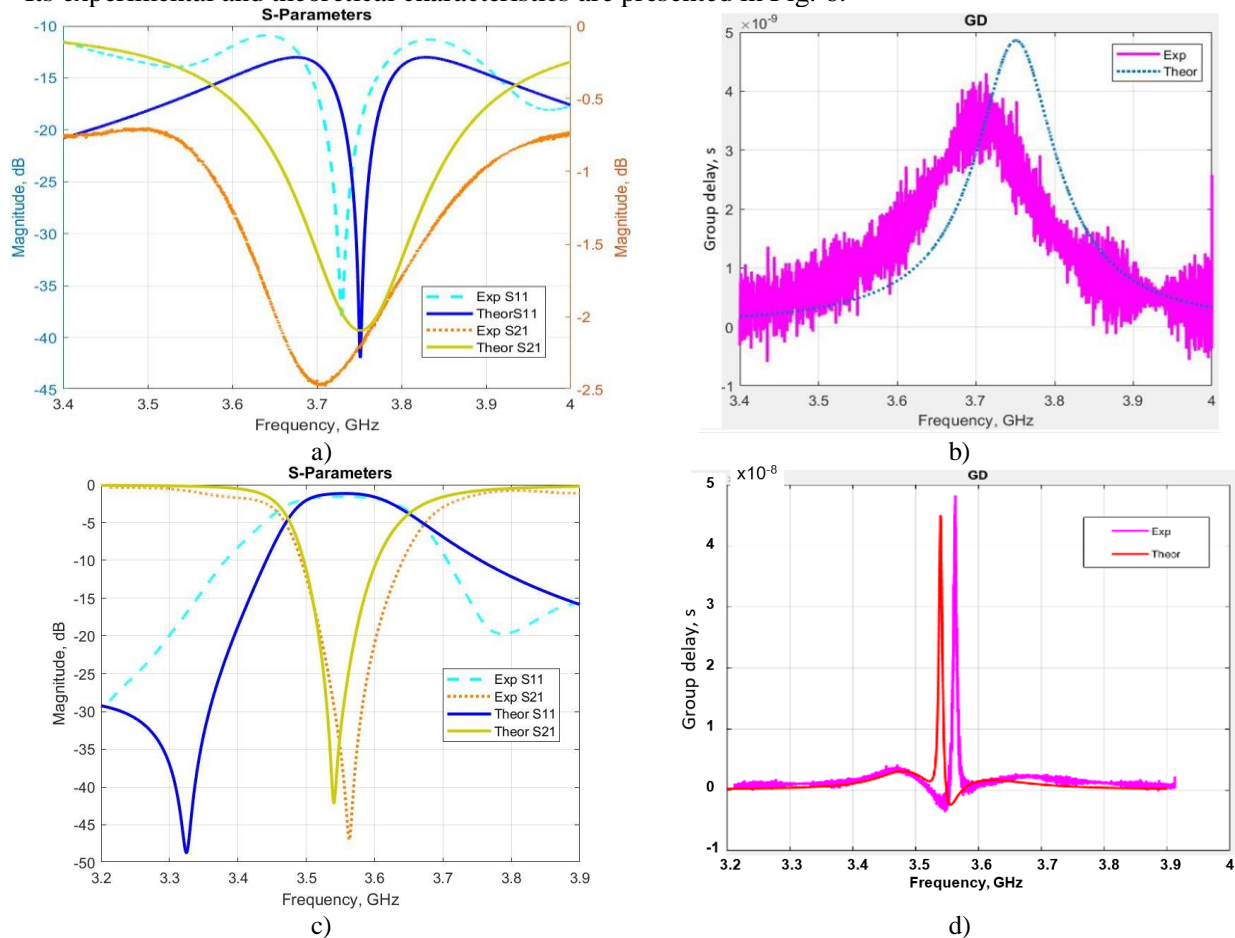


Fig. 6. Experimental and theoretical characteristics of the microstrip filter of Fig. 3 a) - characteristics in Fig. a) and b) - mode of “transparency window”, in Fig. c) and d) - mode of Fano resonance

Since the unloaded Q-factor of the microstrip resonators are approximately the same ($Q_0 \approx 250$), and the coupling coefficients of the resonators are fixed ($K_1 \approx K_2 \approx 7 \pm 1$) and cannot be adjusted, the tuning of the minimum-loss mode (coincidence of the resonant frequencies of the short and long resonators) was achieved with a symmetric reflection coefficient characteristic (Fig. 6 a). The classical “transparency window” in the form of loss reduction at the resonant frequency is not observed (both experimentally and theoretically), and the GD of the metamaterial cell is less than the GD of the individual resonators. This can be seen from the characteristics shown in Fig.7(a) and obtained on the basis of dependences (1) - (12). The loss of the all-pass filter is approximately of 2.5 dB in the phase corrector (equalizer) mode is associated with small values of the Q-factor of microstrip resonators. Fig.7(b) shows the calculated characteristics of a metamaterial cell with typical parameters of its constituent resonators ($Q_0 \approx 250$) to demonstrate both the maximum achievable parameters of such structures and to illustrate the following fact - the frequency of the Fano resonance (attenuation peak on the blue curve S₂₁) coincides with the frequency, at which the red and green characteristics of the stored losses of individual resonators intersect, which indicates the following - the Fano resonance is reached at the point where a complete exchange of energy between individual resonators is possible (without transmitting some difference of the stored energy to the output).

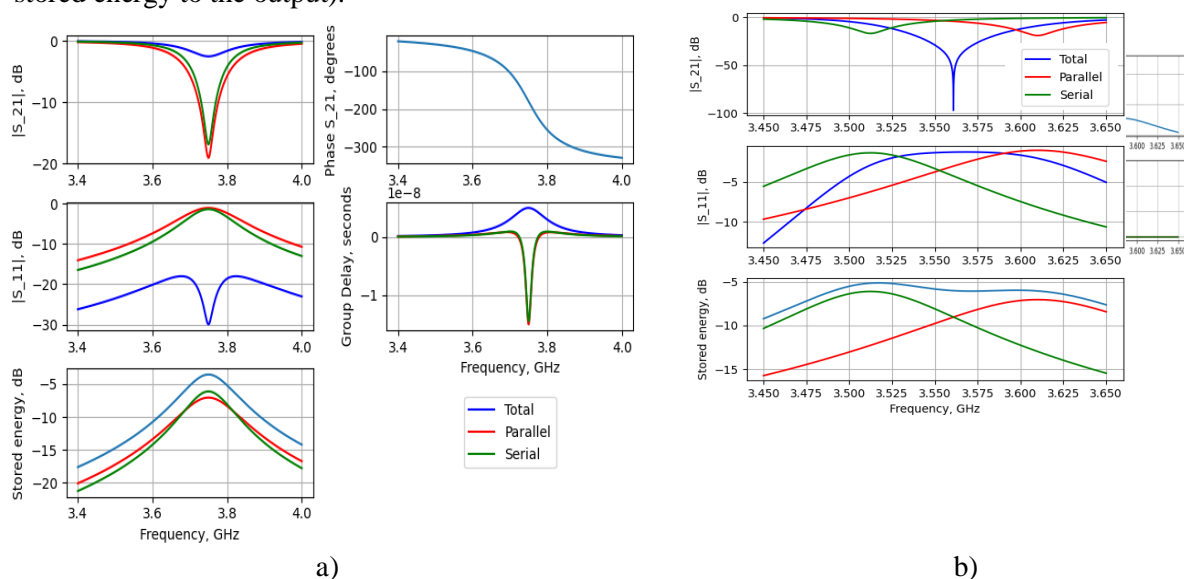


Fig. 7. Calculated characteristics of the microstrip metamaterial cell (presented in Fig.3(b)): a) in the minimum loss mode (“transparency window”); b) in the case of anomalously high attenuation (of about - 100 dB) and GD (of about 30 μ s).

Conclusion

As we can see, the substitution scheme of the all-pass filter on lumped elements, used mainly as an equalizer, allows to model not only its phase and time (GD) characteristics, but also such exotic characteristics of the phenomenon as Fano resonance, EIT and “super-quality”. Theoretically and experimentally demonstrated the most important feature of this kind of structure – the ability to “accumulate” in the matching mode all the incident incoming energy (while each of the resonators cannot “accumulate” more than half of the incident energy) due to the exchange of energy between the resonators in the direction “transverse” to the direction of energy propagation. It is also shown that the GD characteristic of the structure in the “transparency window” mode is a compromise between its maximum values and losses. At the same losses of individual resonators and the structure, the delay time of the system doubles, which can be regarded as a doubling of the system quality compared to the quality of the resonators forming it.

Acknowledgment

This work was supported in part by the National Research Foundation of Ukraine through the Framework of “Microwave Devices Based on Resonant Structures with Metamaterial Properties for the Life Protection and Information Security of Ukraine” under Project 2021.01/0030 and by the Swedish

Foundation for Strategic Research within the framework of SSF Project “Electromagnetic metamaterials for communications and sensing” (ID UKR24-0008).

References

1. R. Levy, "Realization of Practical Lumped Element All-Pass Networks for Delay Equalization of RF and Microwave Filters," in *IEEE Transactions on Microwave Theory and Techniques*, vol. 59, no. 12, pp. 3307-3311, Dec. 2011, doi: 10.1109/TMTT.2011.2172809.
2. Yu, Su. "Group Delay Variations in Microwave Filters and Equalization Methodologies Master ' s." (2012).
3. S. Bose and K. J. Vinoy, "Group delay engineering using cascaded all pass filters for wideband chirp waveform generation," 2013 IEEE International Conference on Electronics, Computing and Communication Technologies, Bangalore, India, 2013, pp. 1-5, doi: 10.1109/CONECCT.2013.6469308.
4. M. Y. Ilchenko *et al.*, "Modeling of Electromagnetically Induced Transparency With RLC Circuits and Metamaterial Cell," in *IEEE Transactions on Microwave Theory and Techniques*, vol. 71, no. 12, pp. 5104-5110, Dec. 2023, doi: 10.1109/TMTT.2023.3275653.
5. Olexander Zhivkov, Oleg V'yunov, Roman Kamarali, Olexandr Fedorchuk, Gleb Avdeyenko, Volodymyr Stepanenko. Simulation of electromagnetically induced transparency and Autler–Townes splitting in microwave frequency range // Workshop on Microwave Theory and Technology in Wireless Communications (MTTW'23), 4-6 October 2023, Riga, Latvia. <https://mttw.rtu.lv/program/>
6. O. Zhivkov, I. Stoianov, V. Tychynskiy-Martyniuk, I. Galitskiy, K. Shevtsov and R. Kamarali, "Modeling of Microwave and Terahertz Trapped Modes by Circuit Theory Methods," 2023 IEEE International Conference on Information and Telecommunication Technologies and Radio Electronics (UkrMiCo), Kyiv, Ukraine, 2023, pp. 1-6, doi: 10.1109/UkrMiCo61577.2023.10380329.
7. Nakanishi, T., & Kitano, M. (2018). Storage and retrieval of electromagnetic waves using electromagnetically induced transparency in a nonlinear metamaterial. *Applied Physics Letters*, 112(20), 201905. doi:10.1063/1.5035442
8. Nakanishi, T., Kitano, M. (2018). Storage and Retrieval of Electromagnetic Waves in Metamaterials by Dynamical Control of EIT-Like Effect. In: Kamenetskii, E., Sadreev, A., Miroschnichenko, A. (eds) *Fano Resonances in Optics and Microwaves*. Springer Series in Optical Sciences, vol 219. Springer, Cham. https://doi.org/10.1007/978-3-319-99731-5_6
9. Toshihiro Nakanishi, "Storage and retrieval of electromagnetic waves in a metasurface based on bound states in the continuum by conductivity modulation," *Opt. Lett.* 48, 5891-5894 (2023) <https://opg.optica.org/ol/abstract.cfm?URI=ol-48-22-5891>
10. E. G. Cristal, "Analysis and Exact Synthesis of Cascaded Commensurate Transmission-Line C-Section All-Pass Networks," in *IEEE Transactions on Microwave Theory and Techniques*, vol. 14, no. 6, pp. 285-291, June 1966, doi: 10.1109/TMTT.1966.1126251.
11. R. Crane, "All-Pass Network Synthesis," in *IEEE Transactions on Circuit Theory*, vol. 15, no. 4, pp. 474-478, December 1968, doi: 10.1109/TCT.1968.1082861.
12. H. W. Bode, *Network Analysis and Feedback Amplifier Design*. New York, NY, USA: D. Van Nostrand Company Inc., 1945.
13. Bechhoefer, J. (2011). Kramers–Kronig, Bode, and the meaning of zero. *American Journal of Physics*, 79(10), 1053–1059. doi:10.1119/1.3614039
14. E. Kamenetskii et al. (eds.), *Fano Resonances in Optics and Microwaves*, Springer. Series in Optical Sciences 219, https://doi.org/10.1007/978-3-319-99731-5_5
15. Hsu, C. W., Zhen, B., Stone, A. D., Joannopoulos, J. D., & Soljačić, M. (2016). "Bound states in the continuum." *Nature Reviews Materials*, 1(9). doi: 10.1038/natrevmats.2016.48.
16. O. Glubokov, O. Zhivkov, V. Stepanenko, M. Ilchenko and J. Oberhammer, "On Modelling of Balanced Filters," 2024 IEEE International Microwave Filter Workshop (IMFW), Cocoa Beach, FL, USA, 2024, pp. 183-186, doi: 10.1109/IMFW59690.2024.10477116.
17. Ilchenko, M., Zhivkov, A. (2019). Bridge Equivalent Circuits for Microwave Filters and Fano Resonance. In: Ilchenko, M., Uryvsky, L., Globa, L. (eds) *Advances in Information and Communication Technologies. UKRMICO 2018. Lecture Notes in Electrical Engineering*, vol 560. Springer, Cham. https://doi.org/10.1007/978-3-030-16770-7_14
18. Bode, H. W. (1940). Relations Between Attenuation and Phase in Feedback Amplifier Design. *Bell System Technical Journal*, 19(3), 421–454. doi:10.1002/j.1538-7305.1940.tb00839.x